Journal of Sound and Vibration (2000) **233**(4), 643–668
doi:10.1006/jsvi.1999.2837, available online at http://www.idealibrary.com on IDEAL®

ESTIMATION OF ACOUSTIC SOURCE STRENGTH BY INVERSE METHODS: PART I, CONDITIONING OF THE INVERSE PROBLEM

P. A. Nelson and S. H. Yoon

Institute of Sound and Vibration Research, University of Southampton, Southampton SO17 1BJ, England

(*Received* 23 *October* 1998, *and in final form* 15 *December* 1999)

This paper deals with the discrete inverse problem in acoustics. It is assumed that a number of acoustic sources are located at known spatial positions and that the acoustic pressure is measured at a number of spatial positions in the radiated field. The transfer functions relating the strengths of the acoustic sources to the radiated pressures are also assumed known. In principle, the strengths of the acoustic sources can be deduced from the measured acoustic pressures by inversion of this matrix of transfer functions. The accuracy of source strength reconstruction (in the presence of noise which contaminates the measured pressures) is crucially dependent on the conditioning of the matrix to be inverted. This paper examines the conditioning of this inverse problem, particularly with regard to the geometry and number of sources and measurement positions and the non-dimensional frequency. A preliminary investigation is also presented of methods such as Tikhonov regularization and singular value discarding which can improve the accuracy of source strength reconstruction in poorly conditioned cases. Results are also presented which enable the solution of the inverse problem when the time histories of the acoustic sources are time-stationary random processes and the spectra and cross-spectra are measured at a number of positions in the radiated field. The paper illustrates the possibilities and limitations of the use of inverse methods in the deduction of acoustic source strength from radiated field measurements.

1. INTRODUCTION

The estimation of the strength of acoustic sources from measurements of their radiated field is a subject which has been studied extensively by acoustical engineers. The most widely studied problem is that of estimating the angular location of a source relative to an array of sensors, specifically with regard to the detection of sources of underwater sound [1]. Here however, we consider in detail the problem of estimating the strength of the components of a source distribution whose position in space is either known or can be modelled with reasonable accuracy. This problem is of most relevance to engineers who wish to better understand sources of sound in order to reduce their output. Considerable effort was directed towards this problem during the 1970s when researchers first became particularly concerned with the accurate location of sources associated with jet engines. For example, Billingsley and Kinns [2] developed an "acoustic telescope" which made use of an array of microphones whose outputs were weighted depending on an assumed source position. These workers deduced the relationship between the power spectrum of the resulting output signal and the cross power spectral distribution of an assumed line source upon which the array is focused. Another approach was that taken by Fisher *et al.* [3], who derived a relationship between the source strength distribution associated with an uncorrelated line

0022-460X/00/240643 + 26 $35.00/0

source and the cross-correlation functions evaluated between microphones located on a polar arc surrounding the source. This work forms the basis of the "polar correlation" technique. Fisher *et al.* demonstrated that the technique was intrinsically unable to resolve sources separated by less than one-half of an acoustic wavelength. A further approach to the source reconstruction problem was that taken by Maynard *et al.* [4] who introduced the use of nearfield acoustic holography (NAH). In this case, the field impinging on an array that is placed close to the region of the source is decomposed into its constituent plane wave components through the use of a wavenumber transform. Subsequent extrapolation of this field to the plane of the source then follows from the solution of the Helmholtz equation in the wavenumber domain. By undertaking measurements in the nearfield source components can be resolved which are separated by distances of much less than one-half wavelength. The implementation of this technique is described in more detail by Veronesi and Maynard [5] and its practical use has been clearly described by Hald [6,7] and Ginn and Hald [8].

In addition to these approaches to the problem, another method for reconstructing an estimate of the source distribution has been used by a number of workers. For example, in a later paper on the polar correlation technique, Tester and Fisher [9] described an "automatic source breakdown technique" which relied on a pre-supposed model of the jet noise source distribution. Tester and Fisher proceeded to find the strengths associated with their model which minimized the difference between the measured cross-spectra of the microphone array signals and those predicted by their model. A very similar approach to the source identification problem was later taken by Filippi *et al.* [10]. These workers introduced a numerical technique which again enabled identification of an *a priori* chosen model for the source distribution. The essence of this approach was to find the distribution of source strength used in the model which minimized a cost function which quantified the mean square error between the measured field and the output of the model. The models used by Filippi *et al.* consisted of either a decomposition of the radiated field into spherical harmonics or a discretized representation of the source distribution in a Kirchoff–Helmholtz representation of the source and sound field. As an example, these workers modelled the radiation from a vibrating beam, expressed the field in terms of spherical harmonics up to sixth order, and deduced the source strengths associated with 19 discrete elements of the beam. They introduced 10% random error into their simulated measurements and studied the accuracy to which the source distribution could be reconstructed as a function of the position of the measurements made. They noted that the technique became more accurate as the measurement array was moved closer to the source distribution. The connection between this type of approach and that of NAH was made by Veronesi and Maynard [11] who also used a discretized version of a Kirchoff–Helmholtz representation of source distributions but for those with arbitrary geometry. A matrix of transfer functions was then defined which related the strengths of these discrete sources to the acoustic pressure at a number of field points. This matrix was then expressed in terms of its singular value decomposition (SVD) and Veronesi and Maynard pointed out the similarity between the matrix operations in the SVD and those used in NAH. The generality of the SVD as a method of relating source and field was subsequently exploited by Borgiotti [12], Photiadis [13] and Elliott and Johnson [14], all of whom made use of the technique to define a set of spatially orthogonal source strength distributions and study the efficiency of their radiation to the far field. Kim and Lee [15] also used the SVD in connection with a Kirchoff–Helmholtz representation of the source and radiated field which enabled the field at a number of discrete points to be expressed in terms of the source distribution at a number of discrete points. These authors used the SVD in order to deal with any ill-conditioning of the matrix to be inverted. The technique was found to be successful in practice when applied to the radiation from a cabinet mounted loudspeaker.

More recently, Stoughton and Strait [16] have studied the use of the least-squares method for the identification of the distribution of source strength associated with a line source and Grace *et al.* [17,18] have studied the aeroacoustic inverse problem of identifying the unsteady surface pressure along a streamlined airfoil from the measurement of the radiated sound field. Grace *et al.* made use of Tikhonov regularization in order to deal with ill-conditioning, although the choice of the regularization parameter in the inversion process was made arbitrarily. Fisher and Holland [19] have also recently made use of the same approach in the identification of the sources of shock-cell noise in supersonic jets, although no explicit use was made of regularization techniques.

In summary therefore, there appear to have been two main categories of approach to the source reconstruction problem. The first category relies on "Fourier transform" relationships between source and field, whilst the second uses what may be described as a "model based" approach although, as pointed out by Veronesi and Maynard [11], there is a close connection between the two methods. It is the second, more general, approach that we study further in this work. In particular, we show that, once the sources are well modelled, the accuracy of source strength reconstruction using this technique is determined entirely by the properties of the matrix of transfer functions used in the model which describes the source and field and the amount of measurement noise. We again use the singular value decomposition to both evaluate the errors in source reconstruction with a given microphone array and to improve the accuracy of reconstruction. In this paper, we firstly reintroduce the analytical basis of the technique with a view to maximizing the accessibility of the work to acoustical engineers. Furthermore, we concentrate on the effect of the geometry of the problem on its conditioning and guidelines are given for the design of microphone arrays which enable good results to be achieved. The paper begins with an introduction to the general least-squares estimation problem and sets out the analytical framework for subsequent analysis using the SVD and other techniques for improving estimation accuracy, such as Tikhonov regularization. We also introduce within this framework a convenient technique for the analysis of source distributions having a stationary random output as a function of time. In particular, we deduce the relationship between cross-spectra measured between microphones in the radiated field and the cross-spectral distribution of the modelled sources.

The main results of this paper demonstrate the influence of the geometrical arrangement of sources and sensors on the conditioning of the problem and in particular the improvements in conditioning produced by making measurements in the near field of the sources. Furthermore, results are presented which show the power of singular value discarding and Tikhonov regularization in enabling good results to be achieved even when the problem is poorly conditioned. We also show, however, that the use of singular value discarding also has consequences for the spatial resolution of the technique, and we explain our results in terms of the radiation efficiency of a set of spatially orthogonal source strength distributions which are defined naturally by the SVD. In a subsequent paper, we deal in more detail with methods for improving the conditioning of problems of this type which do not require *a priori* knowledge of the source strength distribution or measurement noise. In particular, we focus on the use of generalized cross validation [20] for choosing either the regularization parameter or the singular values to be discarded.

2. THEORETICAL BACKGROUND

2.1. THE LEAST-SQUARES SOLUTION TO THE ESTIMATION PROBLEM, THE SINGULAR VALUE DECOMPOSITION AND REGULARIZATION METHODS

The basis of the approach is illustrated in Figure 1 which shows a digrammatic representation of both the real source and measurement array and the modelled sources

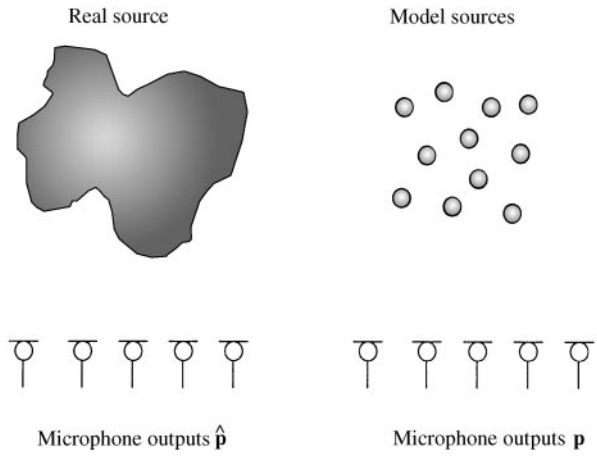

Figure 1. Schematic of the model based approach to source strength estimation.

and modelled measurement array. The output of the model can be written as

$$\mathbf{p} = \mathbf{H}\mathbf{q}, \tag{1}$$

where the vector $\mathbf{p}$ is a complex vector of Fourier transforms of model microphone outputs and the matrix $\mathbf{H}$ is a matrix of complex frequency response functions relating the source strengths in the model to the output of the model microphones. The vector $\mathbf{q}$ is a complex vector of source strength Fourier transforms whose values we wish to determine. Note that in general the nature of the model sources is described by the elements of the matrix $\mathbf{H}$. Thus, for example, if the chosen source model were a combination of monopole and dipole type sources, then the respective monopole and dipole strengths would be defined in the vector $\mathbf{q}$ whilst the radiation patterns of these sources would be defined by the elements of the matrix $\mathbf{H}$. When written in full equation (1) becomes

$$\begin{bmatrix} p_1(\omega) \\ p_2(\omega) \\ \cdot \\ \cdot \\ p_M(\omega) \end{bmatrix} = \begin{bmatrix} H_{11}(\mathrm{j}\omega) & H_{12}(\mathrm{j}\omega) & \cdot\ \cdot & H_{1N}(\mathrm{j}\omega) \\ H_{21}(\mathrm{j}\omega) & H_{22}(\mathrm{j}\omega) & \cdot\ \cdot & H_{2N}(\mathrm{j}\omega) \\ \cdot & \cdot & & \cdot \\ \cdot & \cdot & & \cdot \\ H_{M1}(\mathrm{j}\omega) & H_{M2}(\mathrm{j}\omega) & \cdot\ \cdot & H_{MN}(\mathrm{j}\omega) \end{bmatrix} \begin{bmatrix} q_1(\omega) \\ q_2(\omega) \\ \cdot \\ \cdot \\ q_N(\omega) \end{bmatrix}, \tag{2}$$

where we have assumed that the vector $\mathbf{p}$ is of order M (i.e., there are M microphones), the vector $\mathbf{q}$ is of order N (i.e., there are N sources), and the matrix $\mathbf{H}$ is of order $(M \times N)$. Furthermore, we assume that we have an Mth order vector of *measured* complex Fourier transforms given by

$$\hat{\mathbf{p}}^{\mathrm{T}} = [\hat{p}_1(\omega)\, \hat{p}_2(\omega) \ldots \hat{p}_M(\omega)]. \tag{3}$$

It is now assumed that the measured vector of pressures is equal to the modelled vector of pressures plus a vector $\mathbf{e}$ whose components represent the departure of the measurements from the model and which may include, for example, the effect of contaminating noise.

Thus,

$$\hat{\mathbf{p}} = \mathbf{H}\mathbf{q} + \mathbf{e}. \tag{4}$$

We now seek the solution for the vector $\mathbf{q}$ of modelled source strengths that ensures the "best fit" of the modelled sound field to the measured data. The traditional approach to problems of this type is to find the "least-squares" solution for the complex source strength vector $\mathbf{q}$ which ensures the minimization of the sum of the squared errors ("residuals") between the measured microphone outputs and the model microphone outputs. It is also generally assumed that the number of microphones M is greater than or equal to the number of sources N. The complex error vector can be written as

$$\mathbf{e} = \hat{\mathbf{p}} - \mathbf{p} = \hat{\mathbf{p}} - \mathbf{H}\mathbf{q}, \tag{5}$$

and the cost function for minimization is defined by

$$J = \sum_{m=1}^{M} |e_m(\omega)|^2 = \mathbf{e}^{\mathrm{H}}\mathbf{e}, \tag{6}$$

where the superscript H denotes the Hermitian transpose of a vector (i.e., the complex conjugate of the transposed vector). It is readily shown [21] that the optimal estimate of the source strength vector that minimizes this function is given by

$$\mathbf{q}_0 = \mathbf{H}^{+}\hat{\mathbf{p}}, \tag{7}$$

where $\mathbf{H}^{+} = [\mathbf{H}^{\mathrm{H}}\mathbf{H}]^{-1}\mathbf{H}^{\mathrm{H}}$ is the pseudo-inverse of the matrix $\mathbf{H}$. It can also be shown that this minimum is unique provided that the matrix $\mathbf{H}^{\mathrm{H}}\mathbf{H}$ is positive definite, i.e., provided that $\mathbf{q}^{\mathrm{H}}\mathbf{H}^{\mathrm{H}}\mathbf{H}\mathbf{q} > 0$ for all vectors $\mathbf{q} \neq \mathbf{0}$. Since, in this problem, $\mathbf{q}^{\mathrm{H}}\mathbf{H}^{\mathrm{H}}\mathbf{H}\mathbf{q} = \mathbf{p}^{\mathrm{H}}\mathbf{p}$, which is the sum of the squared magnitudes of the Fourier spectra of the model microphone outputs, we are assured of the positive definitiveness of $\mathbf{H}^{\mathrm{H}}\mathbf{H}$ and the existence of a unique minimum. Note that when the number of microphones M is made equal to the number of modelled sources N, the solution reduces to $\mathbf{q}_0 = \mathbf{H}^{-1}\hat{\mathbf{p}}$. When M is less than N, no solution exists for the source strength vector unless some further constraint is introduced [21].

Now note that we can decompose any arbitrary complex matrix such as the matrix $\mathbf{H}$ into the form [22–24]

$$\mathbf{H} = \mathbf{U}\boldsymbol{\Sigma}\mathbf{V}^{\mathrm{H}}, \tag{8}$$

where in the case $M > N$, the $(M \times N)$ matrix $\boldsymbol{\Sigma}$ is given by

$$\boldsymbol{\Sigma} = \begin{bmatrix} \sigma_1 & 0 & . & . & 0 \\ 0 & \sigma_2 & & & 0 \\ . & . & & & . \\ 0 & 0 & . & . & \sigma_N \\ 0 & 0 & & & 0 \\ . & . & & & . \\ 0 & 0 & . & . & 0 \end{bmatrix}, \tag{9}$$

and comprises the matrix of N singular values σ_n of the $(M \times N)$ matrix $\mathbf{H}$. The matrix $\mathbf{U}$ is of order $(M \times M)$ and its columns comprise the left singular vectors of the matrix $\mathbf{H}$, whilst the matrix $\mathbf{V}$ is of order $(N \times N)$ and its columns comprise the right singular vectors of the matrix $\mathbf{H}$. The matrices $\mathbf{U}$ and $\mathbf{V}$ are unitary and have the properties $\mathbf{U}^{\mathrm{H}}\mathbf{U} = \mathbf{U}\mathbf{U}^{\mathrm{H}} = \mathbf{I}$ and $\mathbf{V}^{\mathrm{H}}\mathbf{V} = \mathbf{V}\,\mathbf{V}^{\mathrm{H}} = \mathbf{I}$. It is usual to arrange the singular values $\sigma_1, \sigma_2 \ldots \sigma_N$ in descending order of magnitude in the matrix defined by equation (9).

Returning to the least-squares solution for the optimal source strength Fourier spectra when the number of microphones M exceeds the number of source elements N, it follows [25] from substitution of equation (8) into equation (7) that

$$\mathbf{q}_0 = \mathbf{V}\boldsymbol{\Sigma}^{+}\mathbf{U}^{\mathrm{H}}\hat{\mathbf{p}}, \tag{10}$$

where the matrix $\boldsymbol{\Sigma}^{+}$ is the pseudo-inverse of $\boldsymbol{\Sigma}$ and can be written as [25]

$$\boldsymbol{\Sigma}^{+} = \begin{bmatrix} 1/\sigma_1 & 0 & . & . & 0 & 0 & . & 0 \\ 0 & 1/\sigma_2 & & & . & . & & . \\ . & . & & & . & . & & . \\ 0 & 0 & . & 1/\sigma_N & 0 & 0 & . & 0 \end{bmatrix}. \tag{11}$$

Thus, any very small singular value will result in large elements of the matrix $\boldsymbol{\Sigma}^{+}$. This in turn will yield very large values of the solution. A traditionally used approach to the stabilization of this solution is simply to discard any small singular values of the matrix $\mathbf{H}$ in computing the source strength estimate given by equation (10). Thus, for example, one simply discards the $(N - D)$ smallest singular values and thus sets the terms $(1/\sigma_N,\ 1/\sigma_{N-1}, \ldots, 1/\sigma_{D+1})$ to zero in the above matrix. We will refer to this matrix as $\boldsymbol{\Sigma}_D^{+}$ where D denotes the number of singular values left after discarding.

Another approach to stabilizing the solution given by equation (10) follows from an alternative definition of the cost function for minimization. Rather than simply minimizing the sum of the squared errors between the measured microphone spectra and the model output spectra we minimize a cost function which also penalizes the sum of the squared model source strengths. We therefore choose to minimize

$$J_R = \mathbf{e}^{\mathrm{H}}\mathbf{e} + \beta\mathbf{q}^{\mathrm{H}}\mathbf{q}, \tag{12}$$

where β is a small regularization parameter.

It is again readily shown [23] that this cost function is minimized by the optimal estimate of the source strength Fourier spectra defined by

$$\mathbf{q}_R = [\mathbf{H}^{\mathrm{H}}\mathbf{H} + \beta\mathbf{I}]^{-1}\mathbf{H}^{\mathrm{H}}\hat{\mathbf{p}}. \tag{13}$$

Use of the SVD in this expression then shows that

$$\mathbf{q}_0 = \mathbf{V}\boldsymbol{\Sigma}_R^{+}\mathbf{U}^{\mathrm{H}}\hat{\mathbf{p}}, \tag{14}$$

where the matrix $\mathbf{\Sigma}_R^+$ is given by [25]

$$\mathbf{\Sigma}_R^+ = [\mathbf{\Sigma}^H\mathbf{\Sigma} + \beta\mathbf{I}]^{-1}\mathbf{\Sigma}^H = \begin{bmatrix} \frac{\sigma_1}{(\sigma_1^2+\beta)} & 0 & . & . & 0 & 0 & . & . & 0 \\ 0 & \frac{\sigma_2}{(\sigma_2^2+\beta)} & . & & 0 & 0 & & & 0 \\ . & . & & . & . & . & & & . \\ . & . & & . & . & . & & & . \\ 0 & 0 & . & \frac{\sigma_N}{(\sigma_N^2+\beta)} & 0 & 0 & . & . & 0 \end{bmatrix}, \quad (15)$$

Thus, any particularly small squared singular value will effectively be increased by the addition of the regularization parameter β and the inversion of the matrix is thus stabilized.

2.2. THE SOLUTION FOR THE SOURCE STRENGTH CROSS-SPECTRA

The analysis leading to equations (10) and (14) above is perfectly general and applicable in practice to acoustic sources that have a deterministic time history (either periodic or transient, for example) which therefore readily yield measurable Fourier spectra. However, in practical acoustics one is often faced with a source strength distribution which has a time dependence that can be regarded as random with stationary statistical properties. In this case, the spectra of the measured acoustic pressure will often be estimated from a series of finite length time histories of random data. Thus, for example, we can define the Fourier spectrum of the ith segment of data of duration T as measured at the mth microphone by

$$\hat{p}_{mi}(\omega) = \int_0^T p_{mi}(t)\, e^{-j\omega t}\, dt, \quad (16)$$

and similarly define the complex vector $\hat{\mathbf{p}}_i$ whose elements are $\hat{p}_{mi}(\omega)$. In addition, we can assume that the modelled acoustic source strengths have analogously defined Fourier spectra $q_{mi}(\omega)$ which comprise the complex vector $\mathbf{q}_i$. One can then deduce the optimal estimate q_{i_0} which minimizes the mean square errors between the ith Fourier spectra measured at the microphones and those deduced from the model. That is we assume $\mathbf{p}_i = \mathbf{H}\mathbf{q}_i$ and minimize $\mathbf{e}_i^H\mathbf{e}_i$ where $\mathbf{e}_i = \mathbf{p}_i - \hat{\mathbf{p}}_i$. This shows that

$$\mathbf{q}_{i_0} = \mathbf{H}^+\hat{\mathbf{p}}_i. \quad (17)$$

We may now formally define the matrix of optimally estimated acoustic source strength auto- and cross-spectra by

$$\mathbf{S}_{qq_0} = \lim_{T\to\infty} E[\tfrac{1}{T}\mathbf{q}_{i_0}\mathbf{q}_{i_0}{}^H], \quad (18)$$

where $E[\ ]$ denotes the expectation operator. It then follows from substitution of equation (17) into equation (18) that

$$\mathbf{S}_{qq0} = \mathbf{H}^+\mathbf{S}_{\hat{p}\hat{p}}\mathbf{H}^{+H}, \quad (19)$$

where we have defined the matrix of measured acoustic pressure auto- and cross-spectra by

$$\mathbf{S}_{\hat{p}\hat{p}} = \lim_{T \to \infty} E[\tfrac{1}{T} \hat{\mathbf{p}}_i \hat{\mathbf{p}}_i^{\mathrm{H}}] \tag{20}$$

In practice of course, this latter quantity is estimated by, for example, averaging over a large (but finite) number of data segments of duration T.

Note that it is also possible to write the solution given by equation (19) in terms of the SVD of the matrix $\mathbf{H}$. It follows directly from the argument presented above that we may write

$$\mathbf{S}_{qq0} = \{\mathbf{V}\boldsymbol{\Sigma}^{+}\mathbf{U}^{\mathrm{H}}\}\mathbf{S}_{\hat{p}\hat{p}}\{\mathbf{V}\boldsymbol{\Sigma}^{+}\mathbf{U}^{\mathrm{H}}\}^{\mathrm{H}}. \tag{21}$$

We may also choose to discard a number of small singular values of the pseudo-inverse matrix $\boldsymbol{\Sigma}^{+}$ and replace this matrix by $\boldsymbol{\Sigma}_D^{+}$ or indeed, replace $\boldsymbol{\Sigma}^{+}$ by its Tikhonov regularized counterpart denoted above by $\boldsymbol{\Sigma}_R^{+}$.

3. CONDITIONING OF ACOUSTIC TRANSFER FUNCTION MATRICES

3.1. SENSITIVITY OF SOLUTIONS TO CONDITION NUMBER

Assume for the moment that we are interested in solving the inverse problem posed when the number of microphones M is equal to the number of source elements N (i.e., the matrix $\mathbf{H}$ is square). The sensitivity of the solution for $\mathbf{q}$ to small deviations or errors in $\mathbf{H}$ and $\hat{\mathbf{p}}$ is determined by the condition number of the matrix $\mathbf{H}$ which has to be inverted. This condition number is usually defined as

$$\kappa(\mathbf{H}) = \|\mathbf{H}\| \, \|\mathbf{H}^{-1}\|, \tag{22}$$

where $\|\mathbf{H}\|$ denotes the 2-norm of the matrix $\mathbf{H}$. (See reference [22] for the definitions of the various matrix norms). The 2-norm of $\mathbf{H}$ turns out to be equal to the largest singular value of $\mathbf{H}$ and is also equal to the square root of the largest eigenvalue of the matrix $\mathbf{H}^{\mathrm{H}}\mathbf{H}$ [22]. Thus, in terms of the singular value decomposition, $\|\mathbf{H}\| = \sigma_{\max}$ and $\|\mathbf{H}^{-1}\| = 1/\sigma_{\min}$, where $\sigma_{\max}$ and $\sigma_{\min}$ are, respectively, the maximum and minimum singular values of $\mathbf{H}$. Therefore, for a square matrix $\mathbf{H}$,

$$\kappa(\mathbf{H}) = \sigma_{max}/\sigma_{min}. \tag{23}$$

A simple argument can be used to demonstrate the importance of the condition number to the sensitivity of the solution $\mathbf{q}_0 = \mathbf{H}^{-1}\hat{\mathbf{p}}$ to errors, for example, in the measurement of $\hat{\mathbf{p}}$. Assume for the moment that small deviations of $\mathbf{p}$ produce small deviations $\delta\mathbf{q}$ in the solution. That is, we assume that $\mathbf{Hq} = \mathbf{p}$ and that

$$\mathbf{H}(\mathbf{q} + \delta\mathbf{q}) = (\mathbf{p} + \delta\mathbf{p}). \tag{24}$$

A useful property of the matrix 2-norms is that $\|\mathbf{A}\ \mathbf{B}\| \leqslant \|\mathbf{A}\| \, \|\mathbf{B}\|$ for two matrices $\mathbf{A}$ and $\mathbf{B}$ [22]. Since $\delta\mathbf{q} = \mathbf{H}^{-1}\delta\mathbf{p}$ it therefore follows that $\|\delta\mathbf{q}\| \leqslant \|\mathbf{H}^{-1}\| \, \|\delta\mathbf{p}\|$. It also follows that $\|\mathbf{p}\| \leqslant \|\mathbf{H}\| \, \|\mathbf{q}\|$ and therefore we can write

$$\|\delta\mathbf{q}\| \, \|\mathbf{p}\| \leqslant \|\mathbf{H}\| \, \|\mathbf{H}^{-1}\| \, \|\delta\mathbf{p}\| \, \|\mathbf{q}\| \tag{25}$$

and using the definition of the condition number shows that

$$\frac{\|\delta \mathbf{q}\|}{\|\mathbf{q}\|} \leqslant \kappa(\mathbf{H}) \frac{\|\delta \mathbf{p}\|}{\|\mathbf{p}\|}. \tag{26}$$

This important and well-established result demonstrates clearly that the sensitivity of the solution for $\mathbf{q}$ is determined by the condition number of the matrix $\mathbf{H}$ to be inverted; a large ratio of maximum to minimum singular value of $\mathbf{H}$ will greatly amplify small perturbations in $\mathbf{p}$. In practical terms, extraneous noise introduced into the measurement of the acoustic pressure will have a disproportionately large effect on the solution for the source strength vector $\mathbf{q}$ if the matrix is "badly conditioned" with a large $\kappa(\mathbf{H})$. A more sophisticated analysis [22] can be used to study the sensitivity of the solution to errors in the matrix $\mathbf{H}$ itself and again, the errors produced in the solution are found to be in proportion to the condition number of $\mathbf{H}$.

When the matrix $\mathbf{H}$ is not square, its condition number is defined by

$$\kappa(\mathbf{H}) = \|\mathbf{H}\| \, \|\mathbf{H}^+\|. \tag{27}$$

The 2-norm of $\mathbf{H}^+$ is given by $1/\sigma_n$, where σ_n is the smallest non-zero singular value of $\mathbf{H}$, and therefore the condition number of a non-square matrix can be written as

$$\kappa(\mathbf{H}) = \sigma_{max}/\sigma_n. \tag{28}$$

It is also easy to show, by using a very similar argument to that presented above for the case of a square matrix $\mathbf{H}$, that the sensitivity to errors in the measurement $\hat{\mathbf{p}}$ of the "least-squares" solution given by equation (7) is also described by equation (26) but with the condition number defined by equation (27).

It is also important to evaluate the dependence upon condition number of the sensitivity of the solution given by equation (21) for the matrix of auto-spectra and cross-spectra of acoustic source strength, this being evaluated from the matrix of auto-spectra and cross-spectra of measured acoustic pressures. In this case, we can again write the solution given by equation (1) in the form

$$\mathbf{S}_{qq} = \mathbf{H}^+ \mathbf{S}_{pp} \mathbf{H}^{+\mathrm{H}} \tag{29}$$

and now assuming that errors $\delta\mathbf{S}_{pp}$ in the measured pressure cross-spectral matrix result in errors $\delta\mathbf{S}_{qq}$ in the source strength cross-spectral matrix shows that

$$\delta\mathbf{S}_{qq} = \mathbf{H}^+ \delta\mathbf{S}_{pp} \mathbf{H}^{+\mathrm{H}}. \tag{30}$$

We can thus use the matrix norm property to write $\|\delta\mathbf{S}_{qq}\| \leqslant \|\mathbf{H}^+\| \, \|\delta\mathbf{S}_{pp}\| \, \|\mathbf{H}^{+\mathrm{H}}\|$. Again using the property of matrix norms in equation (29) shows that $\|\mathbf{S}_{pp}\| \leqslant \|\mathbf{H}\| \, \|\mathbf{S}_{qq}\| \, \|\mathbf{H}^{\mathrm{H}}\|$ and we can therefore write

$$\|\delta\mathbf{S}_{qq}\| \, \|\mathbf{S}_{pp}\| \leqslant \|\mathbf{H}\| \, \|\mathbf{H}^+\| \, \|\mathbf{H}^{\mathrm{H}}\| \, \|\mathbf{H}^{+\mathrm{H}}\| \, \|\mathbf{S}_{qq}\| \, \|\delta\mathbf{S}_{pp}\|. \tag{31}$$

It thus follows:

$$\frac{\|\delta\mathbf{S}_{qq}\|}{\|\mathbf{S}_{qq}\|} \leqslant \kappa(\mathbf{H}) \, \kappa(\mathbf{H}^{\mathrm{H}}) \frac{\|\delta\mathbf{S}_{pp}\|}{\|\mathbf{S}_{pp}\|}. \tag{32}$$

We have again used the definition of the condition number of a non-square matrix **H** given by equation (27), above, and since the ratio of maximum to minimum singular values of **H** will be the same as those of $\mathbf{H}^{\mathrm{H}}$, we can write

$$\frac{\|\delta \mathbf{S}_{qq}\|}{\|\mathbf{S}_{qq}\|} \leqslant \kappa(\mathbf{H})^2 \frac{\|\delta \mathbf{S}_{pp}\|}{\|\mathbf{S}_{pp}\|}. \tag{33}$$

This result, which is generalization to non-square matrices **H** of that first derived in reference [26], demonstrates clearly that the estimation of acoustic source strength auto- and cross-spectra is even more sensitive to errors (because of squared condition number) in the measurement of pressure spectra than when simply attempting to estimate source strength Fourier spectra. This is perhaps not surprising since the auto-spectrum is proportional to the square of the Fourier spectrum and one would expect errors to be equivalently amplified. However, estimating the power spectrum is often the only option in practice and this result emphasizes the need to deal effectively with poorly conditioned problems through the use of regularization methods.

3.2. FACTORS AFFECTING CONDITION NUMBER

The basic characteristics of the discrete inverse problem in acoustics are revealed by studying a simple source/sensor geometry. This is shown in Figure 2 and consists of a linear array of nine-point monopole sources spaced apart from one another by a distance r_{ss}. The same number of sensors are spaced apart by a distance r_{mm} in a line array which is in turn a distance of r_{ms} from the source array. Figure 3 shows a plot of the condition number of the matrix **H** as a function of $kr_{ss} = \omega r_{ss}/c_0$ where ω denotes the angular frequency and c_0 is the sound speed (assumed here to be 344 m/s). The curves shown depict the variation in condition number for a range of values of the ratio r_{ms}/r_{ss}. It is clear that the matrix of transfer functions becomes badly conditioned as both kr_{ss} becomes small and as the distance of the receiving array from the source array becomes large. Figure 4 shows how the nine singular values of the matrix **H** in this case vary with the distance r_{ms} at the particular non-dimensional frequency given by $kr_{ss} = 0{\cdot}366$ (e.g., at a frequency of 200 Hz when $r_{ss} = 0{\cdot}1$ m). It is clear that the singular values decay with distance from the source array

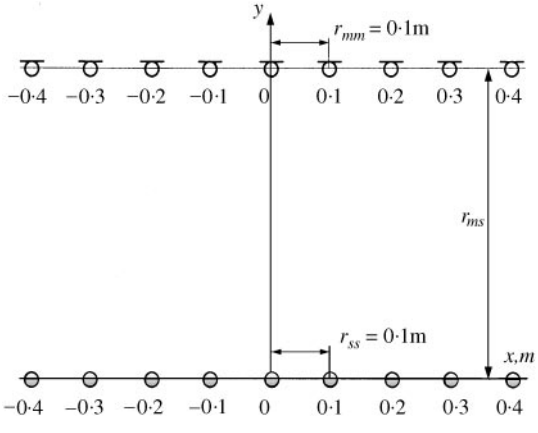

Figure 2. An array of nine-point monopole sources and an array of nine sensors.

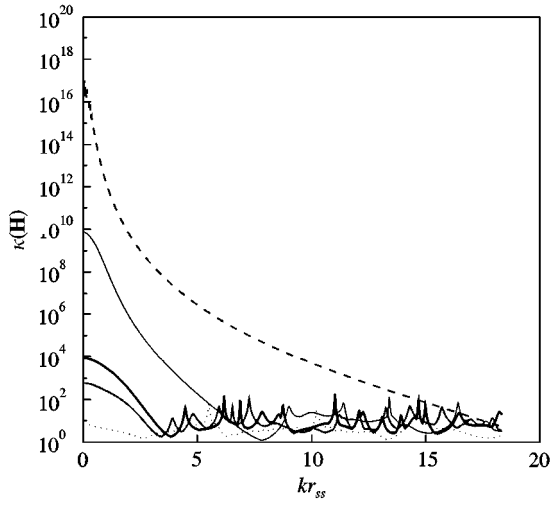

Figure 3. Variation of the condition number of the matrix **H** with the ratio r_{ms}/r_{ss}: dotted: $r_{ms}/r_{ss} = 0{\cdot}5$, grey solid: $r_{ms}/r_{ss} = 2$, black solid; $r_{ms}/r_{ss} = 3$, thin solid: $r_{ms}/r_{ss} = 10$, grey dashed: $r_{ms}/r_{ss} = 30$.

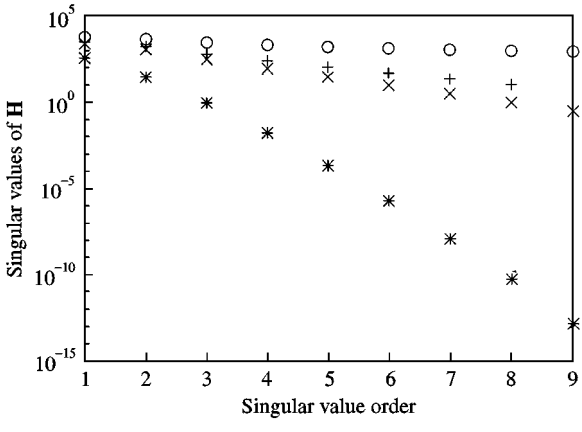

Figure 4. Singular values of the matrix **H** for the model of Figure 2: circle: $r_{ms} = 0{\cdot}5r_{ss}$ ($\kappa(\mathbf{H}) = 5{\cdot}90$), plus, $r_{ms} = 2r_{ss}$ ($\kappa(\mathbf{H}) = 5{\cdot}06 \times 10^{2}$), x-mark: $r_{ms} = 3r_{ss}$ ($\kappa(\mathbf{H}) = 7{\cdot}50 \times 10^{3}$), star: $r_{ms} = 30r_{ss}$ ($\kappa(\mathbf{H}) = 2{\cdot}16 \times 10^{15}$).

such that when, for example, $r_{ms}/r_{ss} = 30$, the smallest singular value has reached a very low value and this results in a large value of condition number.

This behaviour can be understood by making reference to the interpretation given by previous workers [11–14] to the SVD when used in connection with acoustic radiation problems. First, recall that the relationship between the vector of radiated pressures **p** and the vector of acoustic source strengths **q** can be expressed in terms of the SVD of the transfer function matrix **H** such that

$$\mathbf{p} = \mathbf{U}\boldsymbol{\Sigma}\mathbf{V}^{\mathrm{H}}\mathbf{q}. \tag{34}$$

Now note that since the unitary matrix **U** has the property $\mathbf{U}^{-1} = \mathbf{U}^{\mathrm{H}}$, then premultiplication of both sides of this equation by $\mathbf{U}^{-1}$ results in

$$\mathbf{U}^{\mathrm{H}}\mathbf{p} = \boldsymbol{\Sigma}\mathbf{V}^{\mathrm{H}}\mathbf{q}. \tag{35}$$

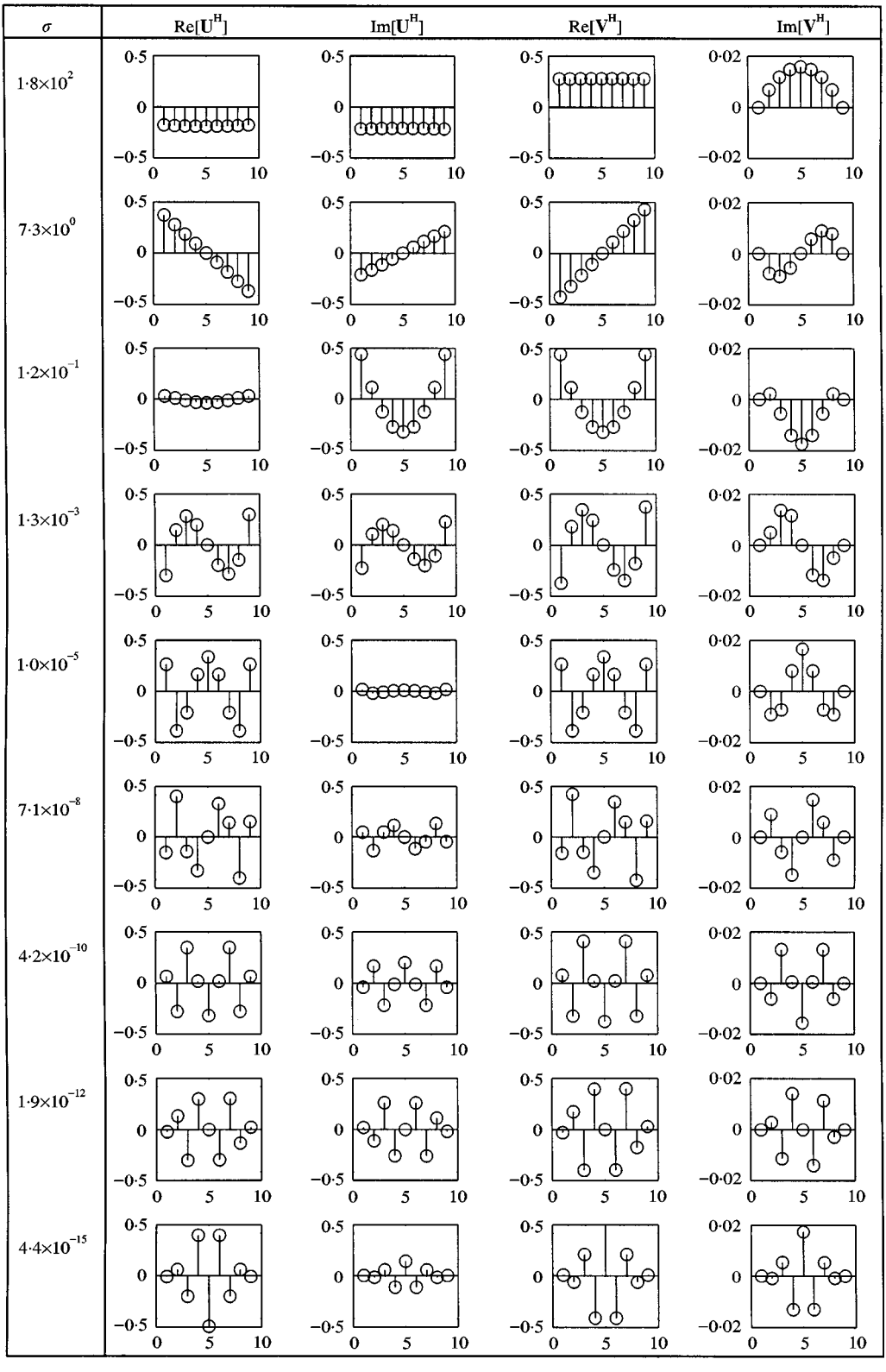
σ
Re[U^H]
Im[U^H]
Re[V^H]
Im[V^H]
1·8×10^2
7·3×10^0
1·2×10^-1
1·3×10^-3
1·0×10^-5
7·1×10^-8
4·2×10^-10
1·9×10^-12
4·4×10^-15
0·5
0
−0·5
0·02
−0·02
0
5
10

We may now interpret $\mathbf{U}^H\mathbf{p} = \tilde{\mathbf{p}}$ as the vector of transformed complex pressures and $\mathbf{V}^H\mathbf{q} = \tilde{\mathbf{q}}$ as the vector of transformed complex source strengths which are related by

$$\tilde{\mathbf{p}} = \mathbf{\Sigma}\tilde{\mathbf{q}}. \tag{36}$$

That is to say, since $\mathbf{\Sigma}$ is a diagonal matrix of real singular values, each element of the vector of transformed pressures is simply related to the corresponding element of the vector of transformed source strengths, the singular values determining the extent to which a given transformed source strength results in the corresponding transformed radiated pressure. As pointed out previously by Veronesi and Maynard [11], Borgiotti [12] and Photiadis [13], the transform operation $\tilde{\mathbf{q}} = \mathbf{V}^H\mathbf{q}$ is somewhat analogous to a Fourier wavenumber transform (of, for example, the surface velocity distribution in a planar radiation problem) whilst the operation $\tilde{\mathbf{p}} = \mathbf{U}^H\mathbf{p}$ is a similar transform of the pressure field (analogous to the Fourier wavenumber transform of radiated pressure in the planar radiation problem). The analogy between this transformation process and that used in planar NAH cannot, however, be pushed too far. The essence of planar NAH is the clear relationship between a given spatial Fourier component of the surface velocity distribution and the corresponding spatial Fourier component in the radiated field pressure; such component either propagate or decay exponentially with distance from the source. In the more general transformation process associated with the SVD it should be noted that the transformation process itself varies with "distance from the source"; the elements of the matrices $\mathbf{U}$ and $\mathbf{V}$ are determined entirely by source/sensor geometry and the transformed pressures and source strengths are related by a single real number (the singular value) which again specifically depends upon geometry.

This transformation process can perhaps be better understood by observing the elements of the matrices $\mathbf{U}$ and $\mathbf{V}$ for the nine source/nine sensor model investigated above. Figure 5 shows the elements of the matrices $\mathbf{U}^H$ and $\mathbf{V}^H$ for the particular value $r_{ms} = 3$ m (i.e., $r_{ms}/r_{ss} = 30$) of distance of the sensor array from the source array and for the non-dimensional frequency $kr_{ss} = 0{\cdot}183$. Note that the rows of $\mathbf{U}^H$ and $\mathbf{V}^H$ define the set of orthonormal basis functions which are at the heart of the transformation process. The spatial distribution of these functions is clear. Note that the rows have been plotted in order of descending singular value and that, at least in this case, the "low spatial frequencies" are associated with large singular values whilst the "high spatial frequencies" are associated with small singular values. A similar plot is shown in Figure 6, but in this case, the source/sensor distance has been reduced to $r_{ms} = 0{\cdot}3$ m (i.e., $r_{ms}/r_{ss} = 3$) although kr_{ss} remains the same as for the case illustrated in Figure 5. Again it is the low spatial frequencies that are associated with the large singular values, although it should be noted that the form of the orthogonal basis functions differs from those illustrated in Figure 5, emphasizing the geometry specific nature of the transformation process. Some further properties of the behaviour of the condition number, in particular its oscillating dependence on frequency are described in more detail in reference [27].

It is therefore evident that in the case studied above, the small singular values are associated with high spatial frequencies. Thus, for example, discarding these small singular values in the process of generating an acceptable solution to the inverse problem, inevitably leads to a deterioration in the spatial resolution of the inversion technique; the reconstructed results

Figure 5. Row elements of the matrices $\mathbf{U}^H$ and $\mathbf{V}^H$ for the source/sensor geometry illustrated in Figure 2 with $r_{ms} = 3$ m ($r_{ms}/r_{ss} = 30$) and $kr_{ss} = 0{\cdot}183$ (100 Hz). The left-hand column shows the singular values of $\mathbf{H}$ corresponding to the rows of $\mathbf{U}^H$ and $\mathbf{V}^H$.

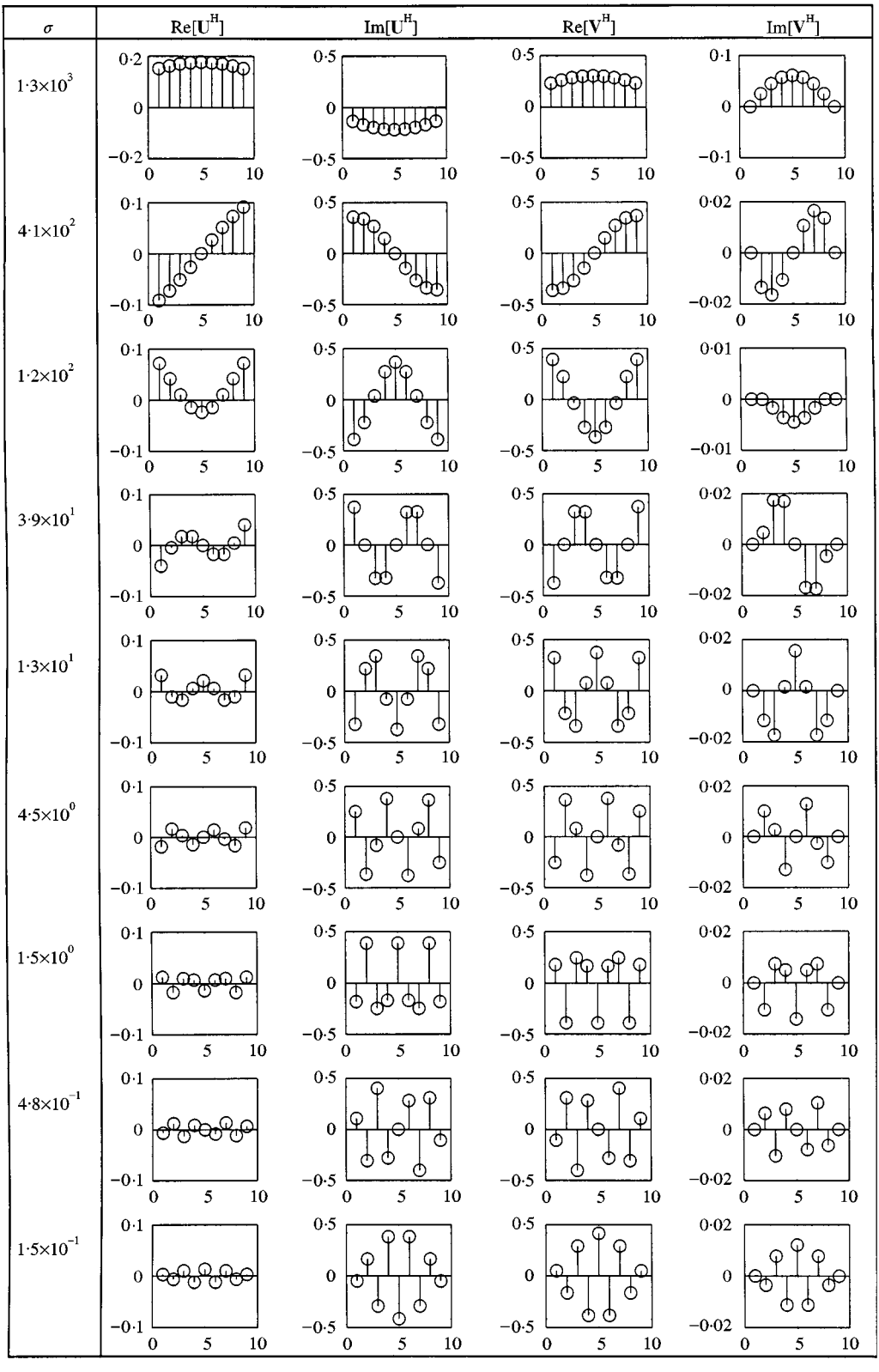
σ
Re[U^H]
Im[U^H]
Re[V^H]
Im[V^H]
1·3×10^3
4·1×10^2
1·2×10^2
3·9×10^1
1·3×10^1
4·5×10^0
1·5×10^0
4·8×10^-1
1·5×10^-1

following the process of singular value discarding are inevitably a "spatially low pass filtered" version of the true source distribution. Whilst it is difficult to be general and each source/sensor geometry must be considered on its own merits, these observations are entirely consistent with the known behaviour of, for example, planar NAH, which requires close deployment of the measurement array in order to capture the evanescent field associated with high spatial frequencies in the source distribution. Measurement arrays deployed far from the source have an intrinsically limited spatial resolution.

3.3. OTHER GEOMETRICAL FACTORS AFFECTING CONDITION NUMBER

A comprehensive study of the influence of the geometric parameters on the condition number is presented in reference [27]. Here we will summarize the main findings of this work. Figures 7–9 show the variation of condition number with a range of parameters for source/sensor geometries consisting, respectively, of linear arrays of six sources and sensors, rectangular arrays of 35 sources and sensors and square arrays of 100 sources and sensors. The dependence is shown on the following parameters:

(1) Non-dimensional frequency kr_{ss}, where r_{ss} is the distance between sources.
(2) Ratio (r_{ms}/r_{ss}) of source plane/sensor plane distance to distance between sources.
(3) Ratio (r_{mm}/r_{ss}) of distance between sensors to distance between sources.
(4) The eccentricity (e) which defines the displacement of the sensor array from a symmetric position relative to the sources.

First note that parts (b) of each of Figures 7–9 demonstrate the important point that, at the particular value of $kr_{ss} = 0{\cdot}55$, the smallest condition number is produced when $r_{mm} = r_{ss}$ and $e = 0$, i.e., the distance between sensors is made equal to the distance between sources. This is particularly so when r_{ms}/r_{ss} is small (i.e., the sensors are close to the sources). Parts (c) and (d) of the figures also demonstrate the effect of the eccentricity e and show that the minimum values of condition number at $r_{mm} = r_{ss}$ are only increased by the displacement of the sensors from the symmetric position. This increase in condition number due to eccentricity is particularly pronounced in the case of a large number of sources and sensors.

Parts (e) of the figures emphasize that $r_{mm}/r_{ss} = 1$ produces a minimum in the condition number for all values of kr_{ss} less than about 2, these plots being produced for specific values of $r_{ms}/r_{ss} = 1$. Finally, parts (f) of the figures again illustrate the dependence of condition number on kr_{ss}, but for a range of values of r_{ms}/r_{ss}, again illustrating the increase of ill-conditioning as r_{ms}/r_{ss} is increased when $e = 0$.

Figure 10 shows the variation of condition number with kr_{ss} for a range of models having increasing numbers of sources and sensors. In all cases $r_{mm}/r_{ss} = 1$ and $r_{ms}/r_{ss} = 1$ and $e = 0$. The plot clearly shows the steady increase of condition number with the increase in the number of sources and sensors used.

Finally, reference [27] describes a series of simulations which investigate the effect of using different sensor array geometries with a given source array geometry. Five different source arrays were chosen (two orthogonal line arrays, a cross array, an X array, and a square array) and in each case the condition number was evaluated for five different sensor

Figure 6. Row elements of the matrices $\mathbf{U}^{\mathrm{H}}$ and $\mathbf{V}^{\mathrm{H}}$ for the source/sensor geometry illustrated in Figure 2 with $r_{ms} = 0{\cdot}3$ m ($r_{ms}/r_{ss} = 3$) and $kr_{ss} = 0{\cdot}183$ (100 Hz). The left-hand column shows the singular values of $\mathbf{H}$ corresponding to the rows of $\mathbf{U}^{\mathrm{H}}$ and $\mathbf{V}^{\mathrm{H}}$.

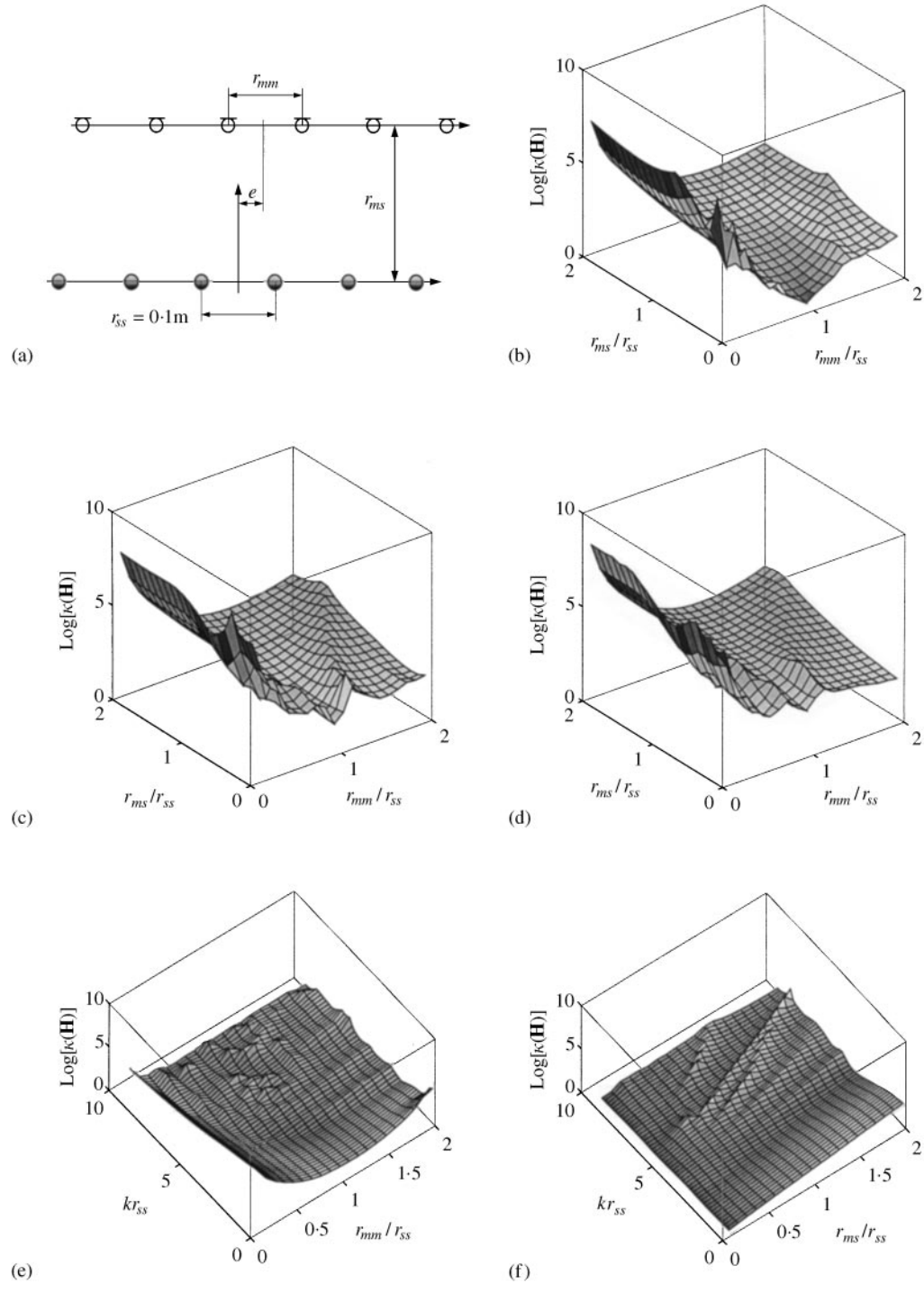

Figure 7. (a) A geometrical arrangement of 6 sources and 6 microphones. Variation of the condition number $\kappa(\mathbf{H})$: (b) $kr_{ss} \approx 0{\cdot}55$ (= 300 Hz), $e = 0$, (c) $kr_{ss} \approx 0{\cdot}55$ (= 300 Hz), $e = -0{\cdot}5r_{ss}$, (d) $kr_{ss} \approx 0{\cdot}55$ (= 300 Hz), $e = 0{\cdot}8r_{ss}$, (e) $r_{ms}/r_{ss} = 1$, $e = 0$, (f) $r_{mm}/r_{ss} = 1$, $e = 0$.

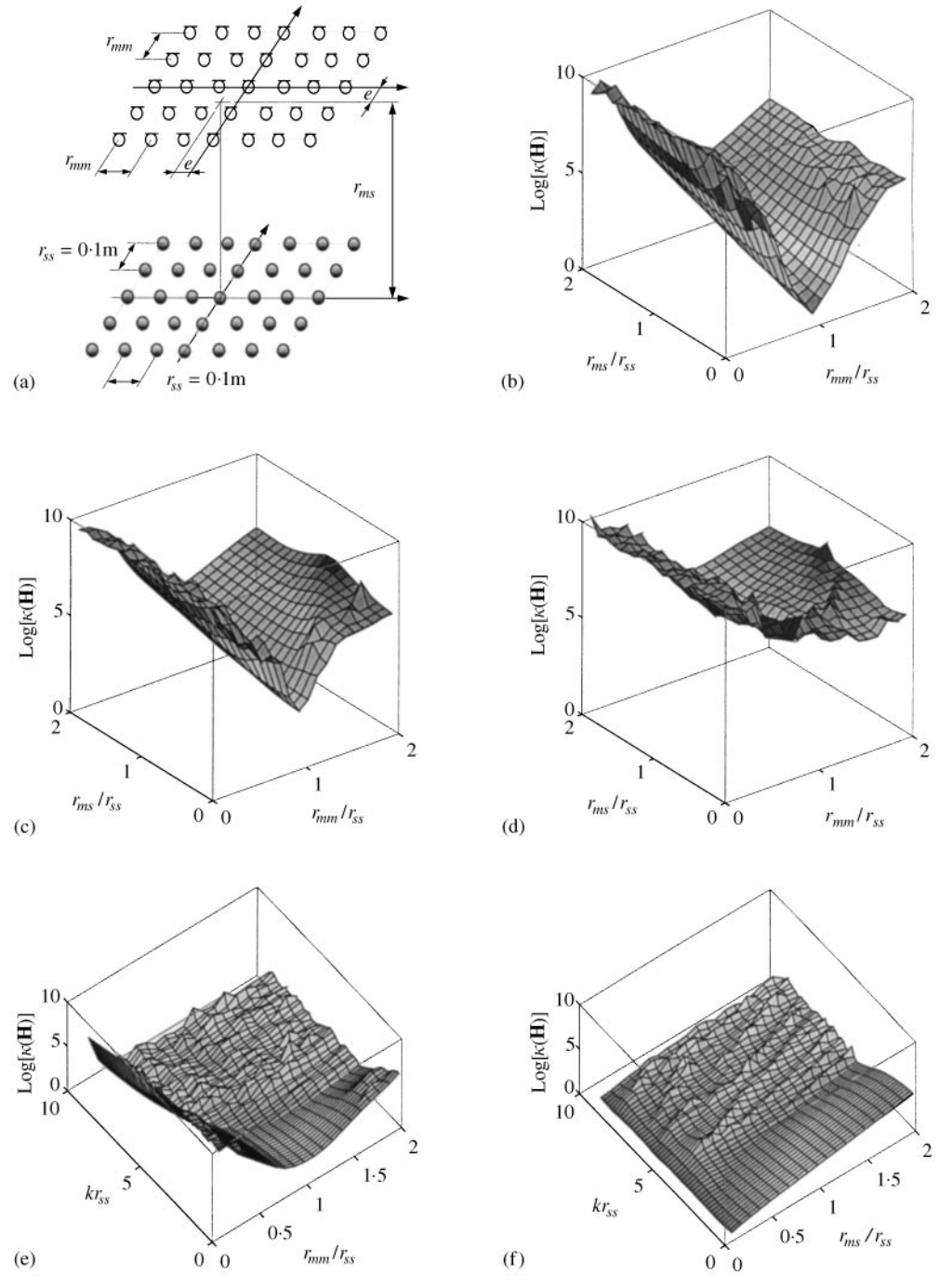

Figure 8. (a) A geometrical arrangement of 35 sources and 35 microphones. Variation of the condition number $\kappa(\mathbf{H})$: (b) $kr_{ss} \approx 0{\cdot}55$ (= 300 Hz), $e = 0$, (c) $kr_{ss} \approx 0{\cdot}55$ (= 300 Hz), $e = -0{\cdot}5r_{ss}$, (d) $kr_{ss} \approx 0{\cdot}55$ (= 300 Hz), $e = 0{\cdot}8r_{ss}$, (e) $r_{ms}/r_{ss} = 1$, $e = 0$, (f) $r_{mm}/r_{ss} = 1$, $e = 0$.

arrays. The consistent finding of these studies was that the condition number was minimized when the geometry of the sensor array exactly matched the geometry of the source array. Two examples are shown in Figures 11 and 12. A remarkable reduction in

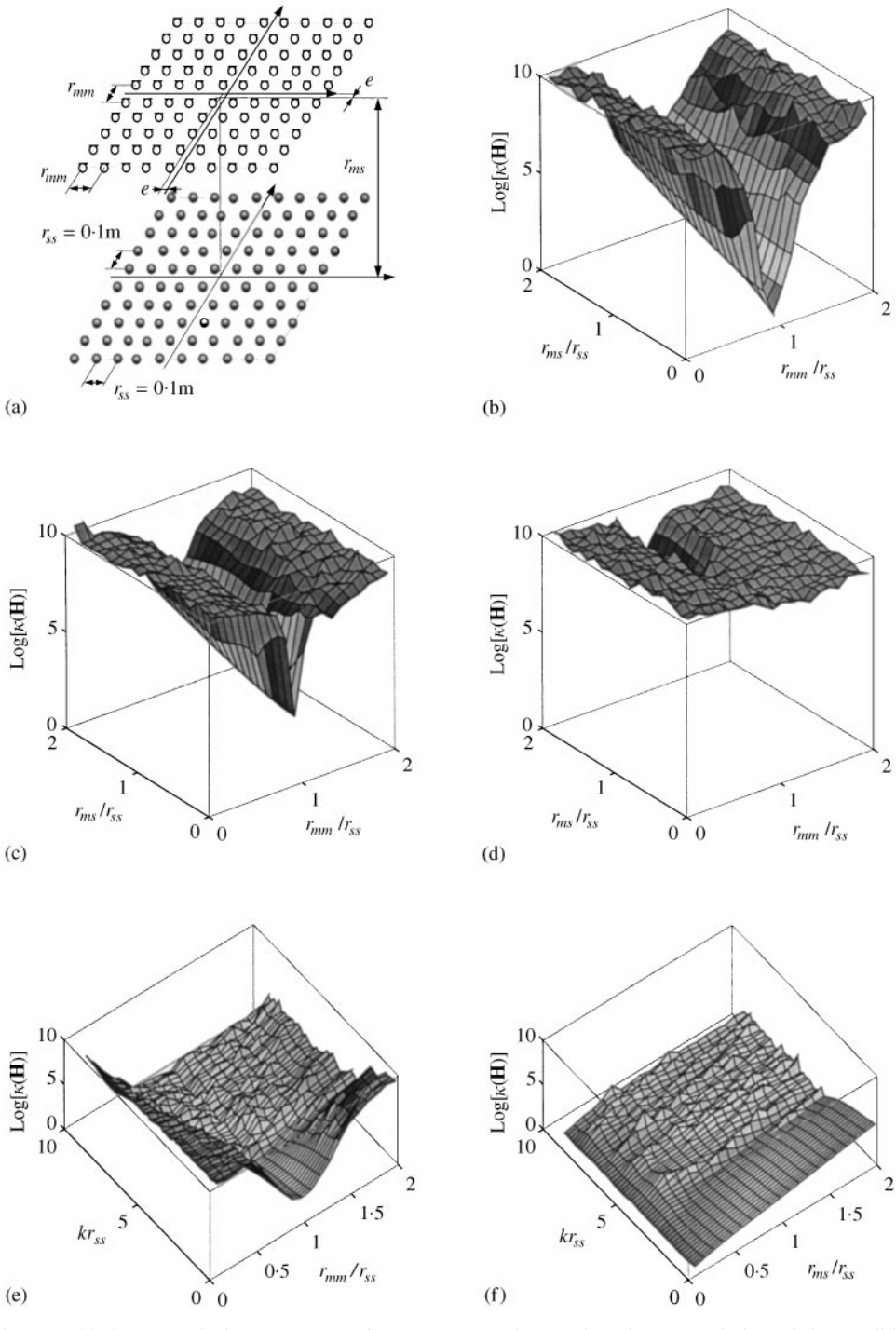

Figure 9. (a) A geometrical arrangement of 100 sources and 100 microphones. Variation of the condition number $\kappa(\mathbf{H})$: (b) $kr_{ss} \approx 0{\cdot}55$ ($= 300$ Hz), $e = 0$, (c) $kr_{ss} \approx 0{\cdot}55$ ($= 300$ Hz), $e = -0{\cdot}5r_{ss}$, (d) $kr_{ss} \approx 0{\cdot}55$ ($= 300$ Hz), $e = 0{\cdot}8r_{ss}$, (e) $r_{ms}/r_{ss} = 1$, $e = 0$, (f) $r_{mm}/r_{ss} = 1$, $e = 0$.

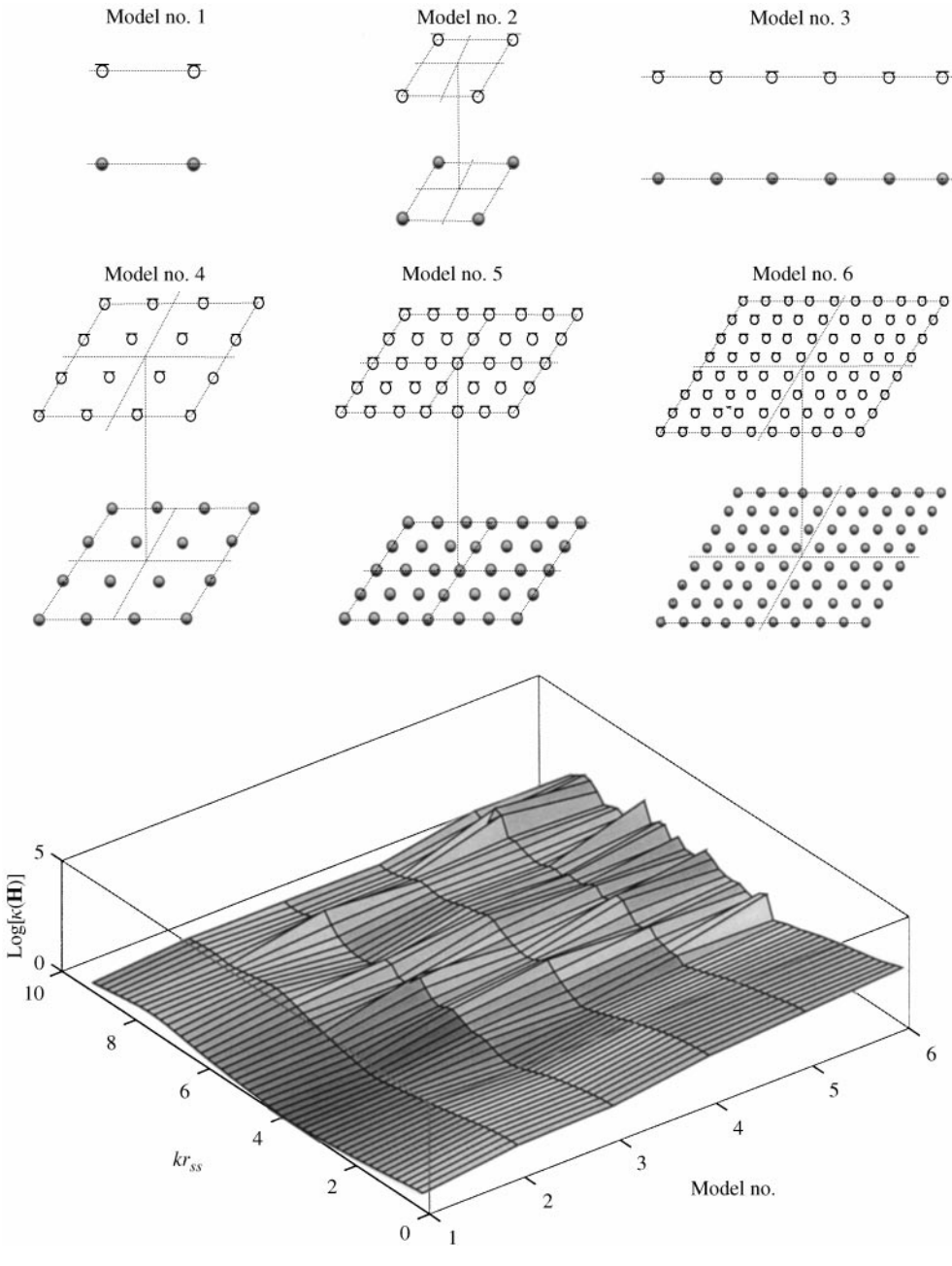

Figure 10. A comparison of condition numbers $\kappa(\mathbf{H})$ of 6 models: $r_{ss} = r_{mm} = r_{ms} = 0{\cdot}1$ m, and the microphone array is placed symmetrically with respect to the source array (i.e., $e = 0$).

condition number is afforded by matching the geometry of the sensor array to the geometry of the source array.

In summary, therefore, the acoustical inverse problem appears to be best conditioned when the number of sources and sensors is small, when the geometrical arrangement of sensors closely matches the assumed source array geometry, when the distance between the sources is the same as the distance between sensors, when the sensor array is placed close to

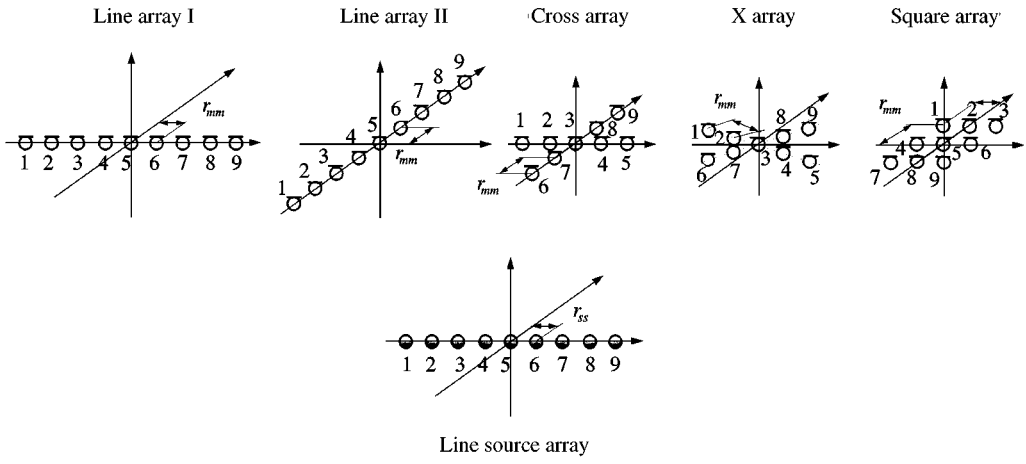

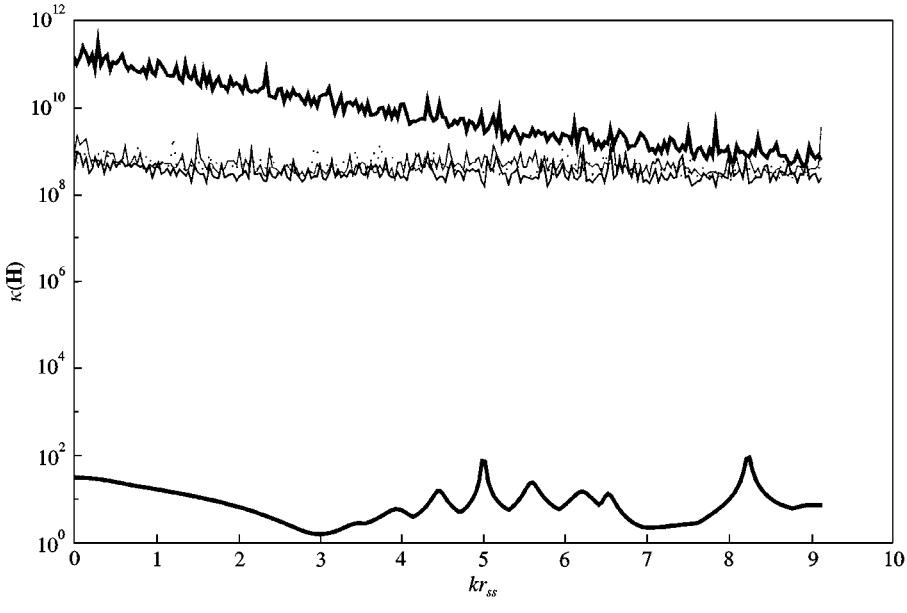

Figure 11. Condition numbers for the five different types of microphone array when used with the line source array. Black thick solid: line microphone array I, grey thick solid: line microphone array II, black thin: microphone array, grey thin: $\times$ microphone array, dotted: square microphone array.

the source array and when the sensor array is positioned symmetrically with respect to the source array.

4. SIMULATIONS OF THE EFFECT OF SINGULAR VALUE DISCARDING AND TIKHONOV REGULARIZATION ON SOURCE RESOLUTION

Following the establishment of general guidelines on the conditioning of the inverse problem, we will now demonstrate how effectively the use of singular value discarding can help retrieve useful solutions for the strength of acoustic sources, despite ill-conditioning of the matrix to be inverted. A series of simple simulations can be used to demonstrate the

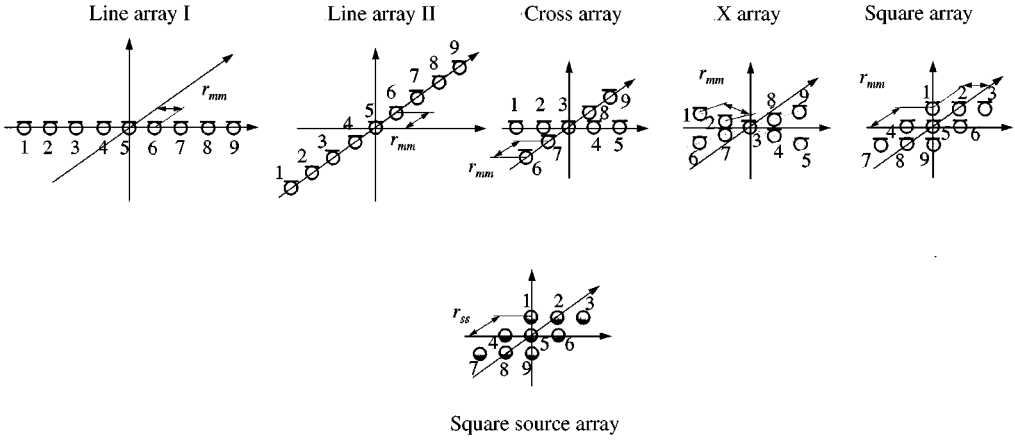

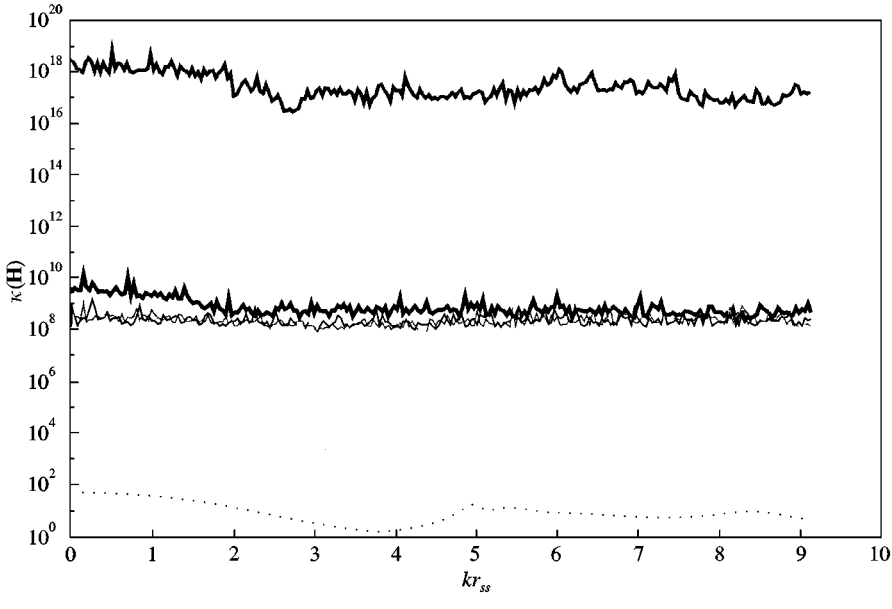

Figure 12. Condition numbers for the five different types of microphone array when used with the source array. Black thick solid: line microphone array I, grey thick solid: line microphone array II, black thin: cross microphone array, grey thin: × microphone array, dotted: square microphone array.

main features of the approach. The geometry dealt with is illustrated in Figure 2 and consists of linear arrays of nine sources and sensors. For the purpose of this exercise it is assumed that the central source in the array has a unit strength, whilst all the other sources are assumed to have a strength of zero.

Figure 13 shows a series of graphs depicting the distribution of source strength deduced from the simulated measured pressure field when the matrix **H** is inverted using singular value discarding. In computing these results it was assumed that $kr_{ss} = 0{\cdot}366$ (i.e., a frequency of 200 Hz when $r_{ss} = 0{\cdot}1$ m). The effects of different levels of noise were simulated by adding random numbers to the "true" pressure field computed for the assumed source distribution. Figure 13 shows results for 10 and 20% random noise and for four

(a)

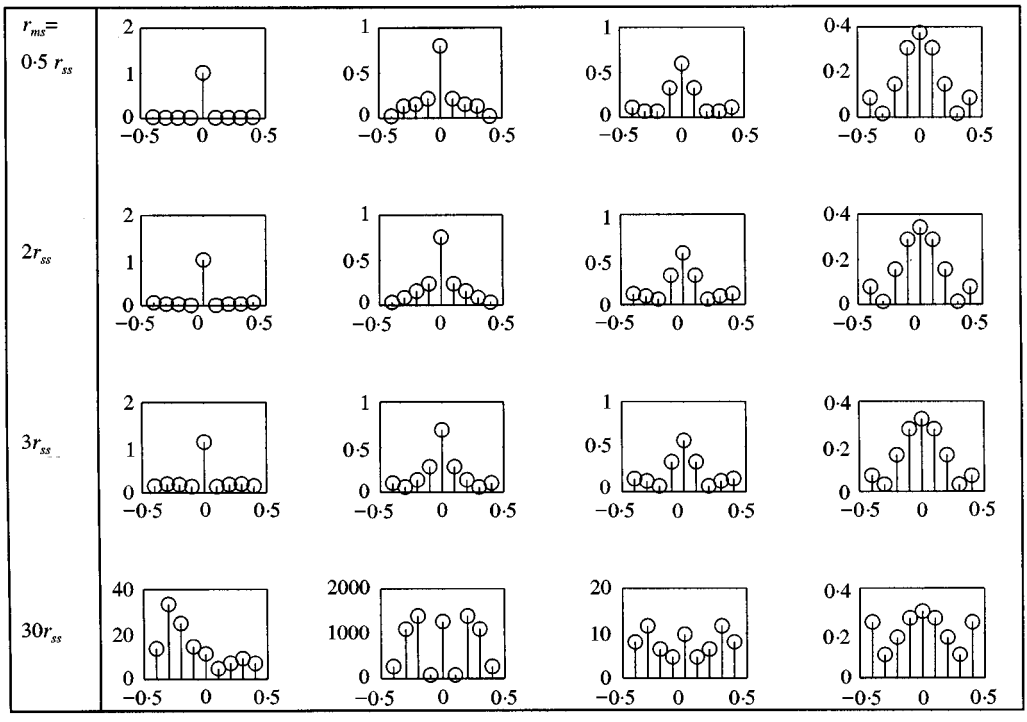

(b)

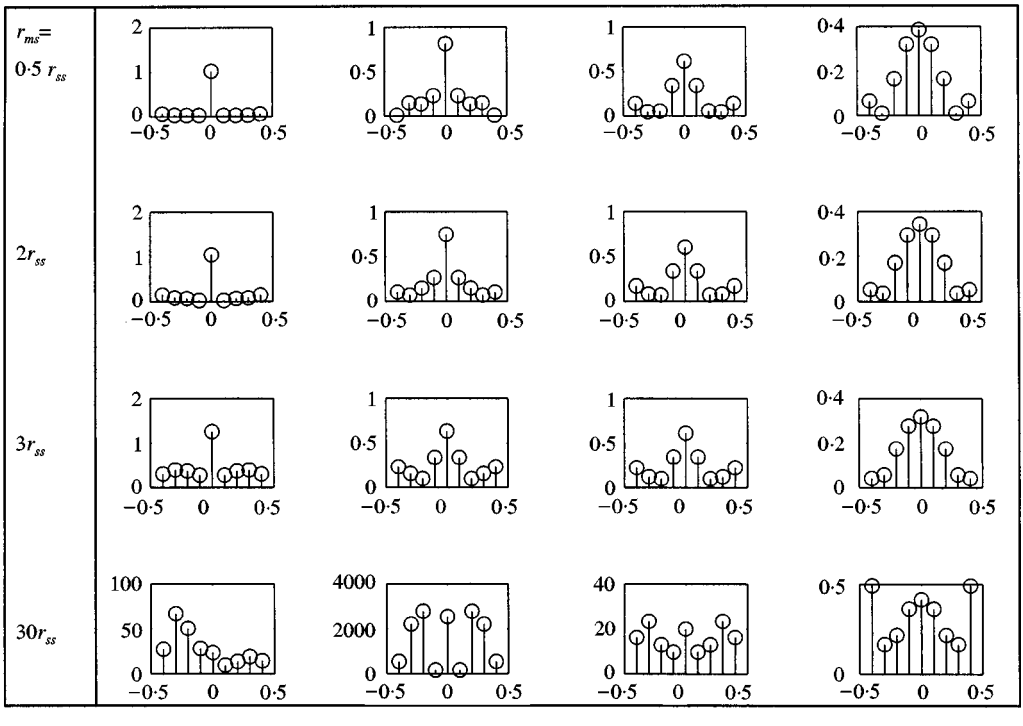

positions of the measurement array relative to the source array ($r_{ms} = 0{\cdot}5r_{ss}$, $2r_{ss}$, $3r_{ss}$, and $30r_{ss}$). The columns of graphs in Figure 13 correspond, respectively, to the cases when none, one, three and five of the smallest singular values of the matrix $\mathbf{H}$ are discarded before computing the solution for the source strength vector $\mathbf{q}_0$.

With reference to the uppermost row of graphs in Figure 13, where $r_{ms} = 0{\cdot}05$ m ($r_{ms} = 0{\cdot}5r_{ss}$) and the problem is well conditioned, it is clear that progressively discarding the singular values of $\mathbf{H}$ gives a progressively poorer spatial resolution of the source strength distribution. Note that very close to the true value of $\mathbf{q}_0$ is recovered, even in the presence of noise, when the problem is well conditioned and no singular values are discarded. However, as the sensor array is moved further from the source array and the conditioning worsens, discarding singular values improves the source strength estimate but at the expense of a decrease in spatial resolution. Thus, for example, in the case of $r_{ms} = 30\ r_{ss}$ (the fourth row of graphs in Figure 13(a)) it can be seen that when no singular values are discarded (the graph in the left-most column) the magnitude of the source strength estimate is seriously in error. This is also true of the graphs in the second and third columns, which correspond, respectively, to the cases where one and three singular values have been discarded. However, once five singular values have been discarded (in the case of the graph in the right-most column), at least the correct order of magnitude of source strength is recovered, although the true source is very poorly resolved spatially. The results shown in Figure 13(b), which correspond to the case where 20% noise is added to the true values, show very similar trends to those of Figure 13(a) which correspond to the addition of 10% noise.

Figure 14 shows the result of Tikhonov regularization of the solution, again for the addition of 10 and 20% noise. Very similar effects are observed to those associated with singular value discarding; the solution when appropriately regularized is capable of retrieving an estimate of the source strength magnitude which is at least of the correct order even if the source strength distribution is not well resolved spatially. It also becomes apparent that choosing too high a value of the regularization parameter β results in even poorer resolution and poorer estimates of the source strength magnitude (see the results in the right-most column of Figure 14). We will return to the choice of an optimal value for β in a later paper.

5. CONCLUSIONS

The conditioning of the discrete inverse problem in acoustics is shown to be highly dependent on the geometry of sources and measurement positions and the frequency of the radiated sound. In particular, the problem generally becomes badly conditioned in the low-frequency limit when the wavelength of the radiated sound becomes large compared to the distance between the sources. However, the conditioning of the problem generally becomes improved when the measurements are made at positions close to the acoustic sources and when the geometry of the measurement positions is chosen to "match" the geometry of the source array. Techniques such as Tikhonov regularization and singular value discarding are shown to be useful methods for improving the accuracy of source strength reconstruction when the problem is poorly conditioned. Methods for choosing the

Figure 13. Resolution capability of the singular value discarding technique for the 9 monopole source and 9 microphone model (Figure 2) with the change of the distance r_{ms} and the singular values discarded. Graphs show the magnitude of $\mathbf{q}_0$ (m^3/s) as a function of position x (m) (Ist column: discarding no singular value, 2nd column: discarding the last singular value, 3rd column: discarding the last 3 singular values, 4th column: discarding the last 5 singular values): $kr_{ss} = 0{\cdot}366$ (= 200 Hz): (a) 10% noise, (b) 20% noise.

(a)

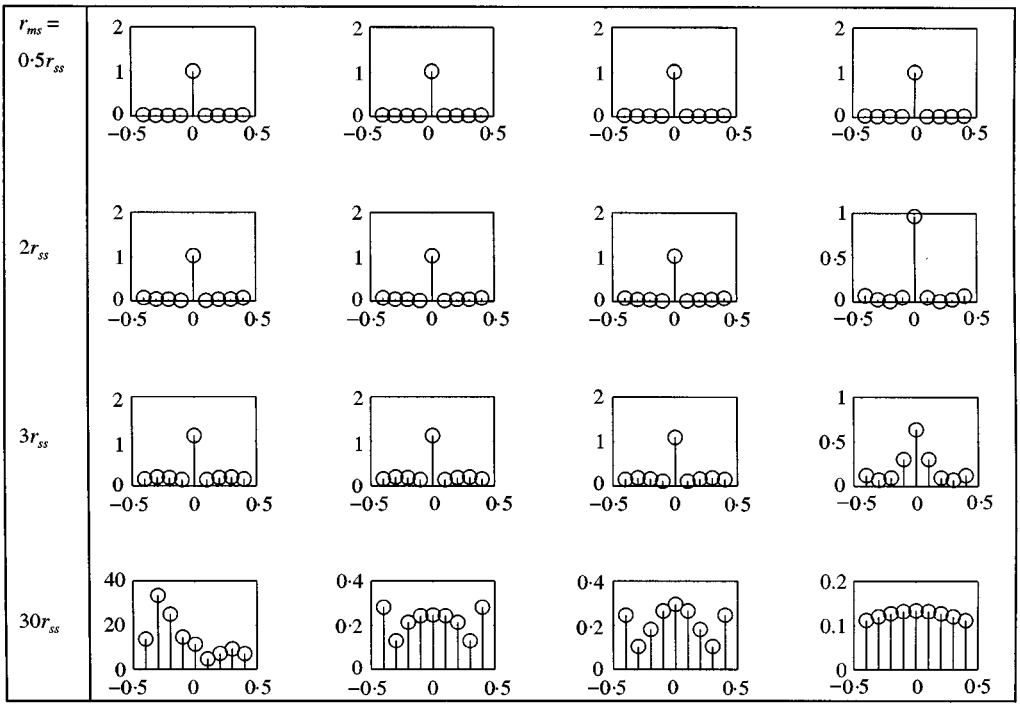
r_{ms} =
$0{\cdot}5r_{ss}$
$2r_{ss}$
$3r_{ss}$
$30r_{ss}$

(b)

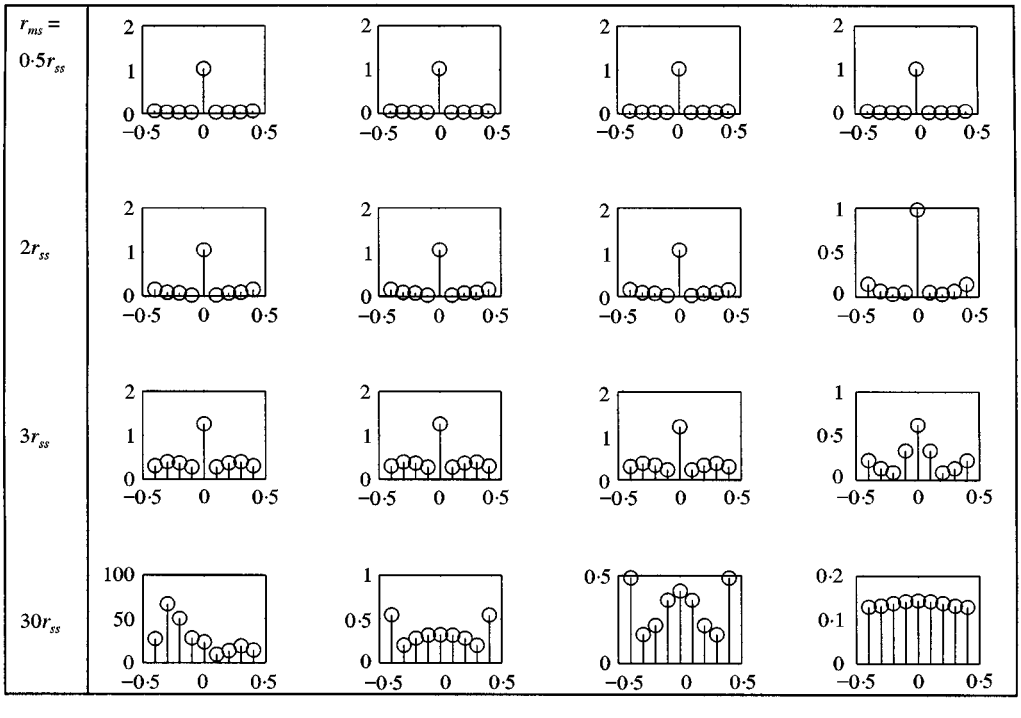
r_{ms} =
$0{\cdot}5r_{ss}$
$2r_{ss}$
$3r_{ss}$
$30r_{ss}$

regularization parameter or the singular values to be discarded will be described in a companion paper together with some experimental results. This paper will also describe techniques for efficiently dealing with acoustic sources whose strengths are a time stationary random processes when measurement of the matrix of cross-spectra of radiated acoustic pressures are required.

REFERENCES

1. B. D. Van Veen and K. M. Buckley 1998 *IEEE ASSP Magazine* 4–24. Beamforming: a versatile approach to spatial filtering.
2. J. Billingsley and R. Kinns 1976 *Journal of Sound and Vibration* **48**, 485–510. The acoustic telescope.
3. M. J. Fisher, M. Harper-Bourne and S. A. L. Glegg 1977 *Journal of Sound and Vibration* **51**, 23–54. Jet engine noise source location: the polar correlation technique.
4. J. D. Maynard, E. G. Williams and Y. Lee 1985 *Journal of the Acoustical Society of America* **78**, 1395–1413. Nearfield acoustic holography: I. Theory of generalised holography and the development of NAH.
5. W. A. Veronesi and J. D. Maynard 1989 *Journal of the Acoustical Society of America* **85**, 588–598. Digital holographic reconstruction of sources with arbitrarily shaped surfaces.
6. J. Hald 1989 *Brüel and Kjær Technical Review No* 1. STSF-a unique technique for scan-based near-field acoustic holography without restrictions on coherence.
7. J. Hald 1995 *Brüel and Kjær Technical Review No* 1. Spatial transformation of sound fields (STSF) techniques in the automotive industry.
8. K. B. Ginn and J. Hald 1989 *Brüel and Kjær Technical Review* 2. STSF-practical instrumentation and application.
9. B. J. Tester and M. J. Fisher 1991 *AIAA 7th Aeroacoustics Conference, Palo Atto, CA, USA*, AIAA-81-2040. Engine noise source breakdown: theory, simulation and results.
10. P. J. T. Fillipi, D. Habault and J. Piraux 1988 *Journal of Sound and Vibration* **124**, 285–296. Noise source modelling and identification procedure.
11. W. A. Veronesi and J. D. Maynard 1989 *Journal of the Acoustical Society of America* **85**, 588–598. Digital holographic reconstruction of sources with arbitrarily shaped surfaces.
12. G. V. Borgiotti 1990 *Journal of the Acoustical Society of America* **88**, 1884–1893. The power radiated by a vibrating body in an acoustic fluid and its determination from boundary measurements.
13. D. M. Photiadis 1990 *Journal of the Acoustical Society of America* **88**, 1152–1159. The relationship of singular value decomposition to wave-vector filtering in sound radiation problems.
14. S. J. Elliott and M. E. Johnson 1993 *Journal of the Acoustical Society of America* **94**, 2194–2204. Radiation modes and the active control of sound power.
15. G. T. Kim and B. H. Lee 1990 *Journal of Sound and Vibration* **136**, 245–261. 3-D sound reconstruction and field projection using the Helmholtz integral equation.
16. R. Stoughton and S. Strait 1993 *Journal of the Acoustical Society of America* **94**, 827–834. Source imaging with minimum mean-squared error.
17. S. P. Grace, H. M. Atassi and W. K. Blake 1996 *American Institute of Aeronautics and Astronautics Journal* **34**, 2233–2240. Inverse aeroacoustic problem for a streamlined body, Part 1: Basic formulation.
18. S. P. Grace, H. M. Atassi and W. K. Blake 1996 *American Institute of Aeronautics and Astronautics Journal* **34**, 2241–2246. Inverse aeroacoustic problem for a streamlined body, Part 2: Accuracy of solutions.
19. M. J. Fisher and K. R. Holland 1997 *Journal of Sound and Vibration* **201**, 103–125. Measuring the relative strengths of a set of partially coherent acoustic sources.

Figure 14. Resolution capability of the Tikhonov regularization technique for the 9 monopole source and 9 microphone model (Figure 2) with the change of the distance r_{ms} and the regularization parameter. Graphs show the magnitude of $\mathbf{q}_0$ (m^3/s) as a function of position x (m). (1st column: $\beta = 0$, 2nd column: $\beta = 1 \times 10^{-5}$, 3rd column: $\beta = 1 \times 10^{-2}$, 4th column: $\beta = 10$): $kr_{ss} = 0{\cdot}366$ (= 200 Hz): (a) 10% noise, 20% noise.

20. G. H. GOLUB, M. HEATH and G. WAHBA 1979 *Technometrics* **21**, 215–223. Generalized cross-validation as a method for choosing a good ridge parameter.
21. P. A. NELSON and S. J. ELLIOTT 1992 *Active Control of Sound*, 416–420. London: Academic Press.
22. G. H. GOLUB and C. F. VAN LOAN 1989 *Matrix Computations*. Baithimore: The John Hopkins University Press, second edition.
23. S. J. ELLIOTT, C. C. BOUCHER and P. A. NELSON 1992 *IEEE Transactions on Signal Processing* **40**, 1041–1052. The behaviour of a multiple channel active control-system.
24. F. DEPRETTERE 1988 *SVD and Signal Processing*. Amsterdam: North-Holland.
25. P. A. NELSON and S. H. YOON 1998 *ISVR Technical Report*, 278 *University of Southampton*. Estimation of acoustic source strength by inverse methods Part I Conditioning of the inverse problem.
26. S. H. YOON and P. A. NELSON 1995 *ISVR Technical Memorandum* 779, *University of Southampton*. Some techniques to improve stability in identifying acoustic source strength spectra.
27. S. H. YOON and P. A. NELSON 1997 *ISVR Technical Memorandum* 817, *University of Southampton*. On the condition number of the matrix to be inverted in an acoustic inverse problem.